

# Quantum-enhanced metrology with single-mode coherent states

Lewis A. Clark, Adam Stokes, and Almut Beige

*The School of Physics and Astronomy, University of Leeds, Leeds LS2 9JT, United Kingdom*

(Dated: September 8, 2022)

In this paper, we show that it is possible to measure the phase shift between two pathways of light with an accuracy above the standard quantum limit without using entanglement. To illustrate this, we propose a quantum-enhanced metrology scheme based on a laser-driven optical cavity inside an instantaneous quantum feedback loop. The purpose of the feedback laser is to provide a reference frame and to enhance the dependence of the dynamics of the system on the measured phase. Since our scheme does not require highly-efficient single photon detectors, it is of practical interest until technologies for the generation of highly-entangled many-photon states become more readily available.

PACS numbers: 06.20.-f, 03.67.Ac, 42.50.Lc, 42.50.Ar

## I. INTRODUCTION

In general, there are two main strategies for reducing the uncertainty in an experimentally measured quantity. One method is to repeat the experiment many times. Another is to use more of an appropriate resource,  $N$ , in every run of the experiment. However, increasing  $N$  is not always possible. Suppose we want to measure a phase shift in light caused by a delicate material, with the help of a standard interference experiment. Increasing the number of photons passing through the sample can increase the accuracy of every phase measurement but also limits the lifetime of the material [1–3]. In this case, it is important that every run of the experiment is as accurate as possible. Using all available resources independently, the scaling of the lower bound of the uncertainty of the phase measurement,  $\Delta\varphi_{\text{class}}$ , is given by the *standard quantum limit*,

$$\Delta\varphi_{\text{class}} \propto N^{-0.5}. \quad (1)$$

Here,  $N$  corresponds, for example, to the total number of independent photons passing through the material. Using the properties of quantum physics and replacing these independent photons by entangled ones, one can improve upon the above limit [4, 5]. The uncertainty of a single phase measurement,  $\Delta\varphi_{\text{quant}}$ , can now be as low as the *Heisenberg limit*,

$$\Delta\varphi_{\text{quant}} \propto N^{-1}, \quad (2)$$

where  $N$  denotes again the total number of photons passing through the sample. The exact form of this limit can vary from experiment to experiment and there is still some discussion over what constitutes a resource, and what form the scaling should take [6, 7].

Achieving the Heisenberg limit usually requires highly entangled photon states as a resource. States that have been discussed in the literature include squeezed states [8, 9],  $N00N$  states [10], twin Fock states [11], pair-coherent states [12–14] and  $mm'$  states [15, 16]. Quantum metrology schemes may then manipulate and measure these states, using techniques such as quantum feedback [17], photon parity measurements [18, 19], probes

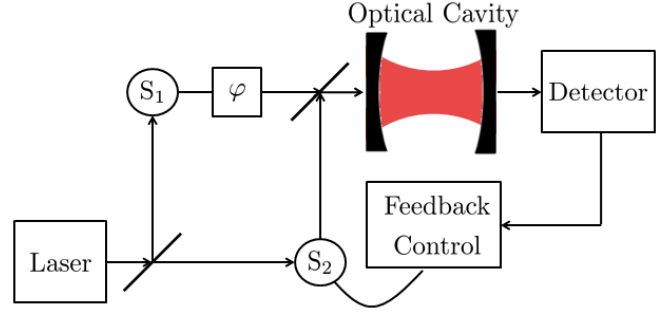


FIG. 1: [Color online] Schematic view of the experimental setup of the proposed two-step measurement of the phase shift,  $\varphi$ , seen by an incoming laser field that drives an optical cavity. The cavity is placed inside an instantaneous feedback loop, which when activated causes the cavity to experience a short laser pulse whenever the spontaneous emission of a photon is detected. The switches,  $S_1$  and  $S_2$  allow the laser-driving to be turned on or off and also control the feedback pulses.

with fluctuating number states [20] and photon subtraction [21]. As well as closed quantum systems, open quantum systems are considered also [22, 23]. A recent review of these matters has been given by Dowling and Seshadreesan [24].

Unfortunately, previous quantum metrology schemes are in general hard to realise experimentally, particularly when the number of photons involved,  $N$ , becomes relatively large [25–27]. To overcome this problem, this paper takes an alternative approach and studies the potential use of single-mode coherent states of light in quantum-enhanced metrology. As we shall see below, improving the accuracy of phase measurements beyond the standard quantum limit does not require entangled photons as a resource [7, 28]. The scheme, which we propose here, might therefore be of some practical interest until technologies for the preparation and manipulation of highly-entangled many-photon states become more readily available.

The experimental setup that we consider in the follow-

ing consists of a single-mode optical cavity. The cavity is either driven by an external laser field or placed inside an instantaneous feedback loop depending on the stage of the experiment, as illustrated in Fig. 1. Our phase measurement scheme consists of two main stages. Firstly, during the preparation stage, the optical switches in Fig. 1 are set such that the external laser experiences the unknown phase shift  $\varphi$  before entering the resonator. The purpose of this stage is to prepare the cavity in a coherent state  $|\alpha(\varphi)\rangle$ , which depends strongly on  $\varphi$ . For simplicity and to assure robustness against dissipation, we suggest that this state is chosen as the stationary state  $|\alpha_{ss}\rangle$  of the resonator. Secondly, during the measurement stage, the optical switches are set such that the cavity only experiences an instantaneous feedback loop. The feedback loop uses the same laser field as the preparation stage and contains a single-photon detector. The detector has a finite efficiency,  $\eta$ , and detects the spontaneous leakage of photons through the cavity mirrors. Whenever a photon is detected, a feedback device closes switch  $S_2$  to send a short and relatively strong pulse into the resonator.

Before the proposed phase measurement can be performed, a calibration stage is needed, which adjusts the interferometer in Fig. 1 and assures that the two paths of light are of the same length when  $\varphi = 0$ . The purpose of the feedback loop is two-fold. Firstly, it provides a reference frame for the measurement of  $\varphi$ . Secondly, it causes the dynamics of the cavity field to depend very strongly on its initial state  $|\alpha(\varphi)\rangle$ , thereby exposing information about  $\varphi$ . Indeed, it is well known that feedback can significantly alter the dynamics of a quantum system [29, 30]. Applications of quantum feedback already include quantum metrology [17], state preparation schemes [31–33], quantum transport [34] and the realisation of quantum hidden Markov models [35].

The origin of the very strong dependence of the dynamics of the cavity in Fig. 1 on its initial state is due to an interesting effect. Unlike most quantum optical systems with spontaneous photon emission, the electromagnetic field inside the resonator never reaches its stationary state. The reason for this is that the stationary state of the cavity is *not* a statistical mixture of coherent states. However, being initially in a coherent state, the cavity can be shown to remain in a coherent state at all times. As we shall see below, the experimental setup in Fig. 1 evolves in a manner that resembles the chaotic behaviour of classical systems [36]. Its dynamics depends very strongly on the initial state  $|\alpha(\varphi)\rangle$  of the resonator, which is what allows us to perform better-than classical phase estimation.

In the following we assume that an experimenter determines the probability density to detect the emission of a photon a time  $T$  after the detection of a photon at the start of the measurement stage. Such a measurement constitutes a measurement of the second-order photon correlation function  $g^{(2)}(T, 0)$ , which does not require highly-efficient single photon detectors. Moreover, as we

shall see below, second-order photon correlations yield information about the phase  $\varphi$  with an accuracy  $\Delta\varphi$ , which exceeds the standard quantum limit. The fact that photon correlation measurements can give better-than classical results has already been noticed before. In Refs. [37, 38], Oppel *et al.* and Pearce *et al.* discuss how to enhance the resolution in imaging experiments with higher-order photon correlation measurements.

To identify the main resource,  $N$ , of our metrology scheme, we adopt the same approach as Zwiernitz *et al.* [6] and assume that  $N$  can be considered equivalent to the query complexity of the scheme. Essentially, each time the phase  $\varphi$  is probed one resource  $N$  is consumed. By continuously observing the leakage of photons through the cavity mirrors, we probe the unknown phase  $\varphi$  at each time step of the measurement stage. As illustrated in Fig. 2, every time step can be seen as one query posed and hence as providing one resource count. The amount of time  $T$ , which the system spends within the measurement stage during each repetition of the experiment, is therefore a resource. To calculate  $\Delta\varphi$  as a function of  $T$ , we simulate a relatively large number of quantum trajectories of the experimental setup in Fig. 1 and then use the error propagation formula given by

$$\Delta\varphi = \frac{\Delta M}{\left| \frac{\partial M}{\partial \varphi} \right|}, \quad (3)$$

where  $M$  denotes the relevant measurement signal. Here,  $\Delta M$  denotes the uncertainty (or resolution) of  $M$ , while the visibility  $|\partial M / \partial \varphi|$  tells us how sensitive  $M$  is to changes in  $\varphi$ . For completeness and to allow for a fair comparison with other quantum metrology schemes, we also consider the mean number of photons passing through the unknown phase  $\varphi$  as a resource  $N$ . In our scheme, this number essentially equals the mean number of photons  $|\alpha_{ss}|^2$  inside the resonator at the end of

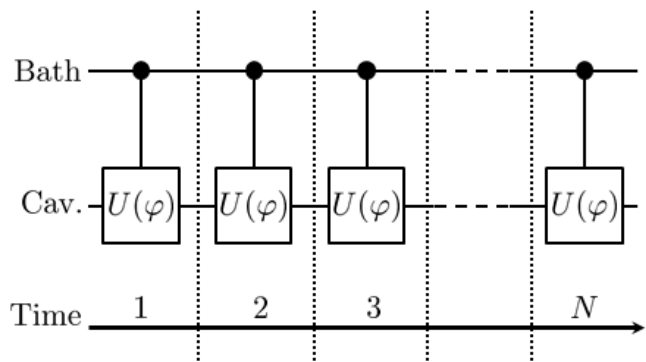


FIG. 2: Circuit diagram of the time evolution of the experimental setup in Fig. 1 during the measurement stage. The black dots indicate that the bath is measured in every time step,  $n = 1, \dots, N$ , and when a photon emission is detected triggers the operator  $U(\varphi)$  to act on the cavity. This process provides information about the state of the cavity and the unknown phase,  $\varphi$ .

the preparation stage. For both resources,  $N = T$  and  $N = |\alpha_{ss}|^2$ , we predict a significant enhancement of  $\Delta\varphi$  beyond the standard quantum limit.

There are five sections in this paper. In Section II, we discuss how to model open quantum systems with and without instantaneous feedback, thereby providing the theoretical background for our work. In Section III we analyse the dynamics of a laser-driven optical cavity with instantaneous quantum feedback in the form of very short strong laser pulses. It is shown that the cavity always remains in a coherent state if it is initially prepared in a coherent state, like the vacuum state. In Section IV, we design a quantum-enhanced metrology scheme with single-mode coherent states. We then calculate its accuracy with respect to intensity measurements, and with respect to second-order photon correlation measurements. Finally we summarise our findings in Section V.

## II. THEORETICAL BACKGROUND

In this section, we give a brief introduction to the modelling of open quantum systems [29, 35, 39, 40]. To do so, we consider a general quantum system, which interacts with a surrounding bath. This reservoir is assumed to also interact with an external environment, which causes the reservoir to thermalise. This means that the environment constantly resets the reservoir into its environmentally preferred state – its so-called pointer state [41, 42]. When coupling to such a reservoir, the time evolution of the open quantum system is approximately Markovian. As such, the dynamics of its density matrix  $\rho_S$ , obey a master equation in Lindblad form [43]. Since the bath surrounding the quantum system is continuously monitored by the environment for the detection of spontaneously emitted photons [44–46], this master equation can be unravelled into an infinite set of physically-meaningful quantum trajectories. Considering such an unravelling, and assuming that the instantaneous feedback is triggered by sudden changes of the state of the reservoir, it becomes very clear how to incorporate instantaneous feedback into the master equation.

### A. Master equations without feedback

Let us first have a closer look at an open quantum system without feedback.

#### 1. Hamiltonian of system and bath

In the following, we describe the quantum system and its reservoir by its Hamiltonian,  $H$ , which can be split it into two parts,

$$H = H_0 + H_1. \quad (4)$$

Here  $H_0$  denotes the free energy of the quantum system and its bath,

$$H_0 = H_S + H_B, \quad (5)$$

while  $H_1$  consists of two terms

$$H_1 = H_{\text{int}} + H_{\text{SB}} \quad (6)$$

where  $H_{\text{SB}}$  describes system bath interactions, and  $H_{\text{int}}$  describes internal system dynamics. The prototypical situation consists of a bath comprised of a continuum of bosonic modes. Moving into the interaction picture with respect to  $H_0$ , the Hamiltonian simplifies to  $H_I(t) = U_0^\dagger(t, 0) H_1 U_0(t, 0)$ , which is of the general form

$$H_I(t) = H_{\text{int}I} + H_{\text{SB}I}. \quad (7)$$

In the following, we use this interaction Hamiltonian to obtain the general form of Markovian master equations for open quantum systems.

#### 2. Environmental effects

Suppose the state of the quantum system at time  $t$  is given by the density matrix  $\rho_S(t)$ . Moreover, adopting the ideas of Zurek and Paz [41, 42] and a related approach by Hegerfeldt [44] and Stokes *et al.* [40], we assume in the following that the reservoir surrounding the quantum system is in general in its environmentally preferred state – the so-called einselected state or pointer state – which we denote by  $|0\rangle$ . Hence

$$\rho_{\text{SB}}(t) = |0\rangle \rho_S(t) \langle 0| \quad (8)$$

is the general density matrix of the system and bath at some time  $t$ . As argued in Ref. [41, 42], the pointer state  $|0\rangle$  is environmentally preferred because it minimises the entropy of the bath. Hence the bath only evolves due to system-bath interactions but is invariant with respect to its own dynamics.

Next, we assume that system-bath interactions perturb the state of the bath on a time scale  $\Delta t$ , which is short compared to the time scale given by the effective internal dynamics of the quantum system. During this time interval, the density matrix  $\rho_{\text{SB}}(t)$  evolves via the time evolution operator  $U_I(t + \Delta t, t)$  into a new density matrix  $\rho_{\text{SB}}(t + \Delta t)$  given by

$$\rho_{\text{SB}}(t + \Delta t) = U_I(t + \Delta t, t) |0\rangle \rho_S(t) \langle 0| U_I^\dagger(t + \Delta t, t). \quad (9)$$

Following the discussion in Refs. [40–42, 44], we now assume that environmental interactions subsequently relax the reservoir very rapidly back into its environmentally preferred state. If the environment acts only locally and does not affect the expectation values of the quantum

system, the result of this thermalisation is a new system-bath density matrix

$$\rho_{\text{SB}}(t + \Delta t) = |0\rangle \rho_{\text{S}}(t + \Delta t) \langle 0| \quad (10)$$

with the state of the system given by

$$\rho_{\text{S}}(t + \Delta t) = \text{Tr}_{\text{B}}(\rho_{\text{SB}}(t + \Delta t)) . \quad (11)$$

Effectively, only  $\rho_{\text{S}}(t)$  has evolved over the interval  $\Delta t$ , and its dynamics can be summarised by the master equation

$$\dot{\rho}_{\text{S}}(t) = \frac{1}{\Delta t} [\rho_{\text{S}}(t + \Delta t) - \rho_{\text{S}}(t)] . \quad (12)$$

### 3. Perturbative Expansions

Given a clear time scale separation between the effective inner dynamics of the quantum system and the

relevant system-bath interactions, the right-hand-side of Eq. (12) can be evaluated using second order perturbation theory. To do so, we write the time evolution operator  $U_{\text{I}}(t + \Delta t, t)$  as

$$U_{\text{I}}(t + \Delta t, t) = 1 - \frac{i}{\hbar} \int_t^{t+\Delta t} dt' H_{\text{I}}(t') - \frac{1}{\hbar^2} \int_t^{t+\Delta t} dt' \int_t^{t'} dt'' H_{\text{I}}(t') H_{\text{I}}(t'') . \quad (13)$$

Substituting this equation into Eq. (9) and combining the result with Eqs. (11) and (12), we find that

$$\begin{aligned} \dot{\rho}_{\text{S}}(t) = & -\frac{i}{\hbar} [H_{\text{int I}}(t), \rho_{\text{S}}(t)] - \frac{1}{\Delta t} \frac{1}{\hbar^2} \int_t^{t+\Delta t} dt' \int_t^{t'} dt'' (\langle 0 | H_{\text{SB I}}(t') H_{\text{SB I}}(t'') | 0 \rangle \rho_{\text{S}}(t) + \text{H.c.}) \\ & + \frac{1}{\Delta t} \frac{1}{\hbar^2} \text{Tr}_{\text{B}} \left( \int_t^{t+\Delta t} dt' \int_t^{t'} dt'' H_{\text{SB I}}(t') | 0 \rangle \rho_{\text{S}}(t) \langle 0 | H_{\text{SB I}}(t'') \right) \end{aligned} \quad (14)$$

up to zeroth order in  $\Delta t$ . When deriving this equation, it has been taken into account that  $\Delta t$  is relatively small and that a typical bath has infinitely many degrees of freedom. Therefore, the double integrals in Eq. (14) scale in general as  $\Delta t$ , and not as  $\Delta t^2$ .

### B. Unravelling into quantum trajectories

To incorporate instantaneous feedback [29, 35] into the above master equation, we notice that the application of feedback requires monitoring the bath for triggering signals. Assuming the presence of such measurements on the above introduced time scale  $\Delta t$  allows us to unravel the above master equation into physically meaningful quantum trajectories [44–46]. We denote the (unnormalised) density matrix of the subensemble of quantum systems for which the bath remains in its environmentally preferred state  $|0\rangle$  by  $\rho_{\text{S}}^0(t)$ , and the (unnormalised) density matrix of the subensemble for which the bath changes by  $\rho_{\text{S}}^{\neq}(t)$ . We have then that

$$\dot{\rho}_{\text{S}}(t) = \dot{\rho}_{\text{S}}^0(t) + \dot{\rho}_{\text{S}}^{\neq}(t) , \quad (15)$$

where

$$\begin{aligned} \dot{\rho}_{\text{S}}^0(t) = & -\frac{i}{\hbar} [H_{\text{int I}}(t), \rho_{\text{S}}(t)] \\ & - \frac{1}{\Delta t} \frac{1}{\hbar^2} \int_t^{t+\Delta t} dt' \int_t^{t'} dt'' \\ & \times (\langle 0 | H_{\text{SB I}}(t') H_{\text{SB I}}(t'') | 0 \rangle \rho_{\text{S}}(t) + \text{H.c.}) \end{aligned} \quad (16)$$

and

$$\begin{aligned} \dot{\rho}_{\text{S}}^{\neq}(t) = & \frac{1}{\Delta t} \frac{1}{\hbar^2} \text{Tr}_{\text{B}} \left( \int_t^{t+\Delta t} dt' \int_t^{t'} dt'' \right. \\ & \left. \times H_{\text{SB I}}(t') | 0 \rangle \rho_{\text{S}}(t) \langle 0 | H_{\text{SB I}}(t'') \right) . \end{aligned} \quad (17)$$

Notice that the trace operation in Eq. (11) is independent of the basis in which it is performed. Consequently, the dynamics of  $\rho_{\text{S}}$  does not depend on how the bath is measured.

For very small  $\Delta t$ , Eq. (16) can be written in the more compact form

$$\dot{\rho}_{\text{S}}^0(t) = -\frac{i}{\hbar} [H_{\text{cond}}(t) \rho_{\text{S}}(t) - \rho_{\text{S}}(t) H_{\text{cond}}^{\dagger}(t)] \quad (18)$$

with  $H_{\text{cond}}(t)$  a (non-Hermitian) conditional Hamiltonian of the open quantum system. Assuming that

$\rho_S(t)$  evolves according to the Schrödinger equation with  $H_{\text{cond}}(t)$  yields Eq. (16) via first order perturbation theory in  $\Delta t$ . In other words, if the quantum system is initially in a pure state  $|\psi_S(t)\rangle$ , it remains pure as long as the state of the reservoir does not change due to system bath interactions [44]. Moreover, the probability for the bath to remain in its preferred state for a time  $\Delta t$  equals

$$P_0(\Delta t) = \|U_{\text{cond}}(t + \Delta t, t) |\psi_S(t)\rangle\|^2 = \text{Tr} \rho_S^0(t + \Delta t) \quad (19)$$

where  $U_{\text{cond}}(t + \Delta t, t)$  denotes the time evolution operator

corresponding to  $H_{\text{cond}}(t)$ .

### C. Master equations with instantaneous feedback

Repeating the above derivation of Eq. (14) while assuming that the quantum system experiences a unitary feedback operation,  $R_m$ , with probability  $\eta_m$  whenever the state of the bath is found in  $|m\rangle$  for  $m \neq 0$ , we arrive again at Eqs. (16) and (18) but find that Eq. (17) needs to be replaced by

$$\begin{aligned} \dot{\rho}_S(t) = & \frac{1}{\Delta t} \frac{1}{\hbar^2} \sum_{m \neq 0} (1 - \eta_m) \int_t^{t+\Delta t} dt' \int_t^{t+\Delta t} dt'' \langle m | H_{\text{SB I}}(t') | 0 \rangle \rho_S(t) \langle 0 | H_{\text{SB I}}(t'') | m \rangle \\ & + \frac{1}{\Delta t} \frac{1}{\hbar^2} \sum_{m \neq 0} \eta_m \int_t^{t+\Delta t} dt' \int_t^{t+\Delta t} dt'' R_m \langle m | H_{\text{SB I}}(t') | 0 \rangle \rho_S(t) \langle 0 | H_{\text{SB I}}(t'') | m \rangle R_m^\dagger. \end{aligned} \quad (20)$$

The kind of feedback described in this subsection is often referred to as *instantaneous feedback*, since it acts on a time scale which is much shorter than the time scale given by the internal system dynamics [29].

## III. EXPERIMENTAL SETUP

The experimental setup that we consider in this paper is shown in Fig. 1. It consists of a laser-driven optical cavity, which is monitored by a photon detector with a finite efficiency  $\eta$ . Upon the detection of a photon, a feedback pulse is applied, which changes the state of the electromagnetic field inside the resonator instantaneously, i.e., on a time scale which is much shorter than the time scale given by the free evolution of the cavity field. In the following, we use the results from the previous section to obtain a quantum optical master equation to describe the dynamics of the resonator with and without feedback applied. It is emphasised that the cavity field always remains in a coherent state, independent of whether or not a photon is detected.

### A. The relevant Hamiltonians

The Hamiltonian  $H_0$  in Eq. (5) contains two contributions,  $H_S$  and  $H_B$ . For the experimental setup in Fig. 1,  $H_S$  describes the free energy of the optical cavity,

$$H_S = \hbar \omega_{\text{cav}} c^\dagger c, \quad (21)$$

where  $\hbar \omega_{\text{cav}}$  denotes the energy of a single photon and  $c$  and  $c^\dagger$  are its annihilation and creation operators respec-

tively, with  $[c, c^\dagger] = 1$ . The Hamiltonian  $H_B$  represents the free energy of the surrounding bath modes – the free radiation field. As usual in quantum optics,

$$H_B = \sum_{\mathbf{k}\lambda} \hbar \omega_{\mathbf{k}\lambda} a_{\mathbf{k}\lambda}^\dagger a_{\mathbf{k}\lambda}, \quad (22)$$

where  $a_{\mathbf{k}\lambda}$  denotes the annihilation operator of a single photon with frequency  $\omega_k$  and wave vector  $\mathbf{k}$  and polarisation  $\lambda$ , while  $a_{\mathbf{k}\lambda}^\dagger$  denotes the corresponding creation operator with  $[a_{\mathbf{k}\lambda}, a_{\mathbf{k}'\lambda'}^\dagger] = \delta_{\lambda\lambda'} \delta_{\mathbf{k}\mathbf{k}'}$ .

In addition, we need to specify the Hamiltonian for the internal dynamics of the system and its system-bath coupling,  $H_{\text{int}}$  and  $H_{\text{SB}}$  in Eq. (6). Going straight into the interaction picture with respect to  $H_0$  and applying the usual rotating wave approximation, we find that

$$\begin{aligned} H_{\text{int I}} &= \frac{1}{2} \hbar \Omega (e^{i\varphi} c + e^{-i\varphi} c^\dagger), \\ H_{\text{SB I}} &= \sum_{\mathbf{k}\lambda} \hbar g_{\mathbf{k}\lambda} a_{\mathbf{k}\lambda}^\dagger c + \text{H.c.} \end{aligned} \quad (23)$$

The first Hamiltonian describes the resonant driving of the cavity by an external laser field with the complex laser Rabi frequency  $\Omega e^{i\varphi}$ . Here  $\Omega$  is assumed to be real, while  $\varphi$  specifies the phase of the laser. Moreover,  $H_{\text{SB I}}$  models the exchange of photon excitation between the cavity and the free radiation field with  $g_{\mathbf{k}\lambda}$  denoting the respective coupling constants.

### B. The relevant master equations

Now that we have identified all the relevant Hamiltonians for the experimental setup in Fig. 1, we can substitute

them into Eq. (14). Calculating the respective integrals and absorbing level shifts into the free energy term  $H_0$ , we find that the master equation of a laser-driven optical cavity without feedback equals

$$\begin{aligned} \dot{\rho}_I = & -\frac{i}{2}\Omega [e^{i\varphi}c + e^{-i\varphi}c^\dagger, \rho_I] \\ & + \frac{1}{2}\kappa \left( 2c\rho_Ic^\dagger - [c^\dagger c, \rho_I]_+ \right), \end{aligned} \quad (24)$$

where  $\kappa$  is a positive real number and denotes the spontaneous decay rate of a cavity photon. Now suppose a detector with efficiency  $\eta$  monitors the spontaneous leakage of photons through one of its mirrors. Whenever a photon is detected, a feedback loop is activated and applies a unitary operator  $R$  to the resonator field. Proceeding as suggested in the previous section, we find that the master equation of the cavity equals

$$\begin{aligned} \dot{\rho}_I = & -\frac{i}{2}\Omega [e^{i\varphi}c + e^{-i\varphi}c^\dagger, \rho_I] \\ & + \eta \cdot \frac{1}{2}\kappa \left( 2Rc\rho_Ic^\dagger R^\dagger - [c^\dagger c, \rho_I]_+ \right) \\ & + (1 - \eta) \cdot \frac{1}{2}\kappa \left( 2c\rho_Ic^\dagger - [c^\dagger c, \rho_I]_+ \right) \end{aligned} \quad (25)$$

in the presence of instantaneous feedback. The second line describes subensembles that experience feedback, while the third line corresponds to undetected photon emission events. Simplifying Eq. (25) yields

$$\begin{aligned} \dot{\rho}_I = & -\frac{i}{2}\Omega [e^{i\varphi}c + e^{-i\varphi}c^\dagger, \rho_I] \\ & + \eta\kappa \left( Rc\rho_Ic^\dagger R^\dagger - c\rho_Ic^\dagger \right) \\ & + \frac{1}{2}\kappa \left( 2c\rho_Ic^\dagger - [c^\dagger c, \rho_I]_+ \right). \end{aligned} \quad (26)$$

In the following, we consider instantaneous feedback in the form of a very short strong laser pulse, meaning that  $R$  can be written as

$$R = D(\beta) \quad (27)$$

with  $D(\beta)$  being the displacement operator,

$$D(\beta) = \exp(\beta c^\dagger - \beta^* c). \quad (28)$$

Here  $\beta$  is a complex number, which characterises the strength of the feedback pulse. Without loss of generality we may take  $\beta$  to have any phase we want by absorbing any unwanted phase factor into the definition of the cavity photon annihilation operator  $c$ .

### C. Unravelling into quantum trajectories

We now have all the information needed to analyse the time evolution of the electromagnetic field inside the resonator under the condition of no photon emission and in the case of the detection of a photon. In this subsection, we introduce all the equations needed to numerically simulate all possible quantum trajectories of a laser-driven optical cavity. We show that the electromagnetic field inside a single optical cavity always remains in a coherent state.

#### 1. No photon time evolution

Substituting Eqs. (22)–(23) into Eq. (16) we obtain an equation of the same form as Eq. (18). Comparing both equations yields

$$H_{\text{cond}} = \frac{1}{2}\hbar\Omega (e^{i\varphi}c + e^{-i\varphi}c^\dagger) - \frac{i}{2}\hbar\kappa c^\dagger c. \quad (29)$$

This conditional Hamiltonian describes the dynamics of the cavity field under the condition of no photon emission. The corresponding conditional time evolution operator,

$$U_{\text{cond}}(t + \Delta t, t) = \exp\left(-\frac{i}{\hbar}H_{\text{cond}}\Delta t\right) \quad (30)$$

is given by

$$\begin{aligned} U_{\text{cond}}(t + \Delta t, t) = & \exp\left[-\frac{i}{2}\Omega (e^{i\varphi}c + e^{-i\varphi}c^\dagger)\Delta t\right] \\ & \times \exp\left[-\frac{1}{2}\kappa c^\dagger c\Delta t\right] \end{aligned} \quad (31)$$

up to terms of order  $(\Delta t)^2$ . Calculating the effect of the second exponential in this equation onto a coherent state  $|\alpha(t)\rangle$  is best done using the Fock basis. To apply the first exponential, we use the general properties of displacement operators. In both cases, we find that the result is again a coherent state. Eventually we find that

$$|\alpha(t + \Delta t)\rangle = U_{\text{cond}}(t + \Delta t, t) |\alpha(t)\rangle / \|\cdot\| \quad (32)$$

where

$$\alpha(t + \Delta t) = e^{-\frac{1}{2}\kappa\Delta t} \alpha(t) - \frac{i}{2}\Omega e^{-i\varphi} \Delta t. \quad (33)$$

is the normalised state of the field inside the cavity under the condition of no photon emission in  $(t, t + \Delta t)$ . This equation tells us that

$$\dot{\alpha}(t) = -\frac{1}{2}\kappa \alpha(t) - \frac{i}{2}\Omega e^{-i\varphi} \quad (34)$$

without any approximations. Solving this differential equation for an initial coherent state  $|\alpha(0)\rangle$ , we find that the state of the cavity equals  $|\alpha(t)\rangle$  with

$$\alpha(t) = e^{-\frac{1}{2}\kappa t} \alpha(0) - \frac{i\Omega}{\kappa} \left(1 - e^{-\frac{1}{2}\kappa t}\right) e^{-i\varphi} \quad (35)$$

under the condition of no photon emission in  $(t, t + \Delta t)$ . If no photon is emitted for a relatively long time  $t \gg 1/\kappa$ , then the state of the resonator becomes

$$|\alpha_{\text{ss}}\rangle = \left| -\frac{i\Omega}{\kappa} e^{-i\varphi} \right\rangle. \quad (36)$$

This state is invariant under the no-photon time evolution of the system. Using Eq. (19), the calculations which lead to Eq. (33) moreover reveal that

$$P_0(\Delta t) = \exp[-|\alpha(t)|^2 (1 - e^{-\kappa\Delta t})] \quad (37)$$

is the probability for no photon emission in the short time interval  $(t, t + \Delta t)$ .

## 2. Spontaneous photon emission

To determine the density matrix  $\rho_S^\neq(t)$ , which describes the cavity field immediately after the emission of a photon, we substitute the system bath Hamiltonian  $H_{\text{SBI}}$  in Eq. (23) into Eq. (17). Evaluating all integrals, we find that

$$\dot{\rho}_S^\neq(t) = \kappa c \rho_S(t) c^\dagger \quad (38)$$

within the usual standard approximations. This equation shows that, if the (normalised) state of an optical cavity immediately after an emission,  $|\alpha(t + \Delta t)\rangle$ , is exactly the same as its state before the emission, if it is prepared in a coherent state  $|\alpha(t)\rangle$ ,

$$|\alpha(t + \Delta t)\rangle = |\alpha(t)\rangle. \quad (39)$$

The reason for this is that coherent states are the eigenstates of the photon annihilation operator. However if the emission of a photon successfully triggers a feedback pulse, the state of the cavity changes into

$$|\alpha(t + \Delta t)\rangle = D(\beta) |\alpha(t)\rangle = |\alpha(t) + \beta\rangle \quad (40)$$

with  $D(\beta)$  being the displacement operator in Eq. (28). In the next section, we use this equation as well as Eqs. (35), (37) and (39) to simulate the dynamics of the cavity field numerically. In every time step of the simulation, we test for a photon emission. A further test is performed to decide if feedback is applied or not, while taking into account the likeliness for such an event to occur.

## D. Long term behaviour

Finally, we have a closer look at the stationary states of the master equations (24) and (26) of a laser-driven cavity with and without instantaneous feedback.

### 1. Convergence without Feedback

In the previous subsection, we have seen that the coherent state  $|\alpha_{\text{ss}}\rangle$  in Eq. (36) is invariant under the no-photon time evolution of a laser-driven optical cavity without feedback. Moreover, Eq. (39) shows that this state is also invariant under the emission of a photon. Consequently,  $|\alpha_{\text{ss}}\rangle$  is the stationary state of a laser-driven optical cavity without feedback. Once the cavity reaches this state, it no longer evolves in time. Indeed, one can easily check that the corresponding density matrix

$$\rho_{\text{ss}} = |\alpha_{\text{ss}}\rangle\langle\alpha_{\text{ss}}| \quad (41)$$

solves the equation  $\dot{\rho} = 0$ .

## 2. Divergence with feedback

Combining the stationary state condition  $\dot{\rho} = 0$  with the master equation in Eq. (26), we now calculate the stationary state of the laser-driven optical cavity with instantaneous feedback. From the discussion in the previous subsection, we know that the field inside the resonator in this case too always remains in a coherent state, if initially prepared in a coherent state. This implies that the stationary state, if it exists, has to be of the form

$$\rho_{\text{ss}} = \int_{\mathcal{C}} d\alpha P(\alpha) |\alpha\rangle\langle\alpha|. \quad (42)$$

Essentially, it needs to be a statistical mixture of coherent states  $|\alpha\rangle$  with weighting  $P(\alpha)$ . However, the master equation (26) does not possess a stationary state of this form. From this we conclude that the laser-driven cavity with instantaneous feedback that we consider in this paper never reaches a stationary state. As we shall see in the next section, it exhibits an even richer dynamics than previously assumed [47–49]. For example, when the cavity is initially prepared in a coherent state, the mean number of photons inside the cavity can grow exponentially [36].

## IV. QUANTUM-ENHANCED METROLOGY

Now we have all the tools needed to design and analyse the quantum metrology scheme illustrated in Fig. 1. It consists of three different stages:

1. **The preparation stage.** A continuous laser field experiences an unknown phase shift  $\varphi$  before entering an optical cavity, as illustrated in Fig. 3(a). The main purpose of this stage is to prepare the field inside the resonator in a coherent state, which depends strongly on  $\varphi$ . For simplicity, we assume that the cavity is driven for a time which is relatively long compared to the time scale given by the laser Rabi frequency  $\Omega$  and the cavity decay rate  $\kappa$ . This stage prepares the cavity in the stationary state given in Eq. (41), which corresponds to the coherent state  $|\alpha_{\text{ss}}\rangle$  in Eq. (36). The phase  $\varphi$  is thereby encoded into the phase of  $\alpha^{\text{ss}}$ .
2. **The measurement stage.** Here the continuous laser driving is turned off, so that the optical cavity evolves freely, while experiencing instantaneous feedback pulses, as illustrated in Fig. 3(b). These are triggered by the observation of a spontaneously emitted photon with a finite detector efficiency  $\eta$ . We assume that every feedback pulse displaces the field inside the cavity by an amount  $\beta$ , given by

$$\beta = -i|\alpha_{\text{rms}}|. \quad (43)$$

During the measurement stage, the laser no longer experiences the unknown phase shift  $\varphi$ . Neverthe-

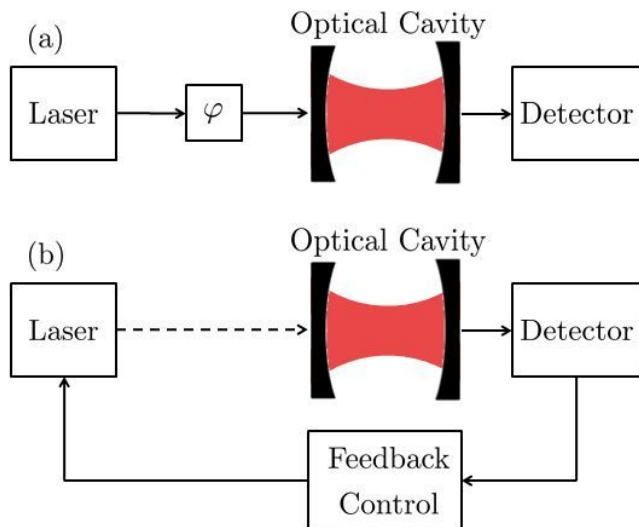


FIG. 3: [Color online] Schematic view of the two main steps involved in the measurement of an unknown phase  $\varphi$ . (a) During the preparation stage, the switches in the experimental setup in Fig. 1 should be set such that the laser experiences this phase before entering the resonator, thereby preparing the cavity in a well-defined coherent state that depends strongly on  $\varphi$ . (b) During the measurement stage, the laser no longer sees  $\varphi$  and a feedback loop is turned on. Whenever a photon is detected, with a finite detector efficiency  $\eta$ , the laser displaces the resonator field with a relatively short and strong pulse. For the feedback to be approximately instantaneous, the duration of the pulse needs to be much shorter than the mean time,  $1/\kappa$ , between photon emission.

less, the photon statistics of the optical cavity reveal information about this phase, because it depends very strongly on the cavity's initial state.

In the following, we consider two different output signals. We either analyse the intensity of the emitted light as a function of time,  $I(T)$ , or the second order correlation function,  $g^{(2)}(T, 0)$ , averaged over many repetitions of the experiment. While measurements of  $I(T)$  allow us to detect  $\varphi$  with an accuracy at the standard quantum limit, measurements of  $g^{(2)}(T, 0)$  yield an accuracy beyond this limit.

3. **Calibration stage.** The purpose of the quantum-enhanced metrology scheme described above is to determine the unknown phase  $\varphi$  with as high a precision as possible. Notice that the outcome of this measurement depends on the difference between the two paths' lengths within the interferometer shown in Fig. 1. It depends on the difference between the phase of the laser field entering the cavity during the preparation stage and the phase of the laser field entering the cavity during the measurement stage. Thus, the proposed scheme needs to be calibrated before it can be applied. We want  $I(T)$  and  $g^{(2)}(T, 0)$  to be as sensitive as possible to small

variations in  $\varphi$ , therefore a control phase may need to be added.

As shown in Fig. 1, changing from one stage to another can be done, for example, with the help of optical switches. In the following, we analyse the accuracy of the proposed quantum-enhanced metrology scheme.

### A. Accuracy of intensity measurements

Let us first discuss how we can deduce the unknown phase  $\varphi$  from measurements of the average photon emission rate  $I(T)$ , where  $T$  denotes the time after the preparation of the cavity field in the initial state in Eq. (41). This means,  $T$  is essentially the minimum length of the measurement stage. To measure  $I(T)$ , we divide the time interval  $(0, T)$  into relatively short time intervals  $\Delta T$ , use the quantum jump approach to simulate a relatively large number of quantum trajectories and average over the respective number of photon emissions in  $(T, T + \Delta T)$ . The result of a numerical simulation of such an experiment for different phases  $\varphi$  is shown in Fig. 4. Looking at this (logarithmic) plot, we see that the dynamics of the mean number of photons inside the resonator depends very strongly on the initial state of the cavity field. This is further illustrated in Fig. 5, which shows a logarithmic plot of  $I(T)$  as a function  $\varphi$  for different times,  $T$ .

In the following, we use this highly non-linear dependence of  $I(T)$  on the unknown phase  $\varphi$  to deduce information about  $\varphi$ . A closer look at Figs. 4 and 5 shows that the dependence of  $I(T)$  on  $\varphi$  is maximised for  $\varphi$  around  $0.3\pi$ . As a manifestation of the relatively chaotic behaviour of optical cavities inside feedback loops, we observe that the curve  $I(T)$  is relatively noisy. Even after averaging over a relatively large number of quantum trajectories, it is difficult to determine the angle that minimises  $\Delta\varphi$ . To calculate the accuracy of the proposed quantum metrology scheme, we consider  $\Delta\varphi$  as a function of  $T$  for  $M = I(T)$  and  $\varphi = 0.3\pi$  as an example. We numerically average again over many quantum trajectories and use the error propagation formula given in Eq. (3). The result of this calculation is shown in Fig. 6. To a very good approximation, we obtain

$$\Delta\varphi(T) \propto T^{-0.49} \quad \text{for } \varphi = 0.3\pi. \quad (44)$$

This means that by performing intensity measurements, the experimental setup in Fig. 1 does not allow us to beat the standard quantum limit in Eq. (1). In fact, we almost saturate this classical limit. This is to be expected as the above described measurement is essentially classical.

### B. Accuracy of second-order correlation function measurements

To see how we can overcome the classical limit, we now calculate how the cavity photon emission rate  $I(0)$



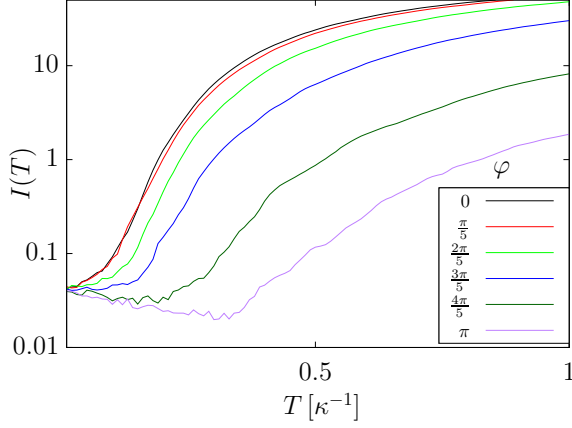


FIG. 4: [Color online] Average intensity,  $I(T)$ , as a function of the time,  $T$ , after the preparation of the initial coherent state,  $|\alpha_{ss}\rangle$ , for various unknown phases,  $\varphi$ . This simulation assumes  $|\alpha_{ss}|^2 = 4$ ,  $\eta = 0.5$  and averages over  $10^6$  trajectories.

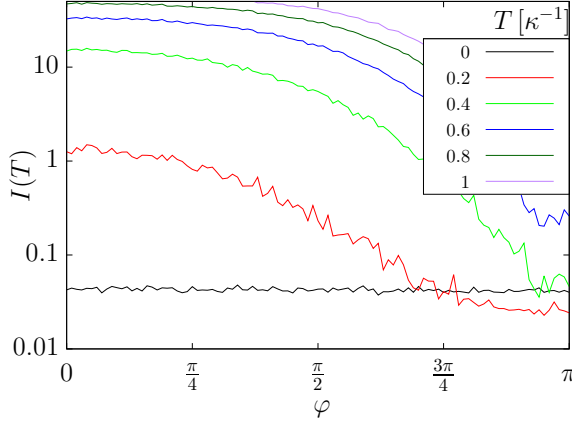


FIG. 5: [Color online] Average intensity,  $I(T)$ , as a function of the unknown phase,  $\varphi$ , for different times,  $T$ . As in Fig. 4, we have  $|\alpha_{ss}|^2 = 4$ ,  $\eta = 0.5$  and average over  $10^6$  trajectories.

changes when instantaneous feedback is added. Using Eq. (43), we see that  $I(0)$  changes from  $\kappa |\alpha_{ss}|^2$  to  $I(0) = \kappa |\alpha_{ss} - i\beta|^2$  in this case. Combining this equation with Eq. (36), we find that

$$I(0) = \frac{4|\Omega|^2}{\kappa} \cos^2\left(\frac{1}{2}\varphi\right) \quad (45)$$

immediately after the detection of a photon at  $t = 0$ . For small angles  $\varphi$ , this expression depends essentially on  $\varphi^2$ . This means, in order to measure an unknown phase  $\varphi$  with the experimental setup in Fig. 1 with a higher-than-classical accuracy, we need to look at higher-order photon correlation functions. Such a function, which can be measured relatively easily experimentally and which has already been considered for quantum imaging applications [37, 38], is the second-order photon correlation

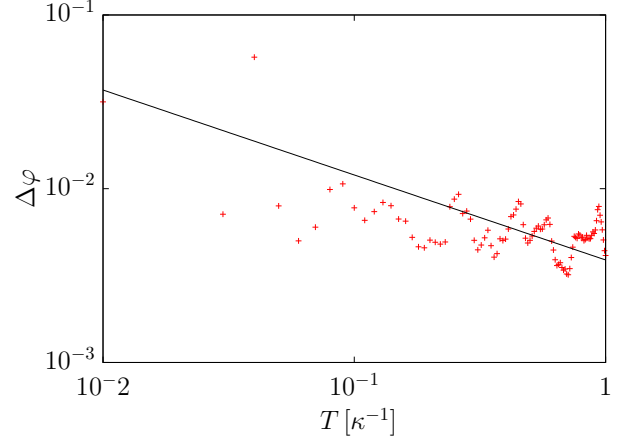


FIG. 6: [Color online] Dependence of the accuracy,  $\Delta\varphi$ , on the length of the measurements stage,  $T$ , in the case of intensity measurements. Here,  $\varphi = 0.3\pi$ ,  $|\alpha_{ss}|^2 = 4$ ,  $\eta = 0.5$  and we averaged over  $10^6$  trajectories. The black line illustrates the approximate solution in Eq. (44).

function  $g^{(2)}(t, t')$ .

The two-time correlation function  $G^{(2)}(t, t')$  associated with the photon statistics of a light source, is defined as the probability to detect a photon at a time  $t$  given the emission of a photon at  $t'$ , i.e.,

$$G^{(2)}(t, t') \equiv I(t|t')I(t'). \quad (46)$$

Second order correlation functions are usually normalised by the respective stationary state photon emission rates. Taking this into account, we now define the renormalised second-order correlation function,  $g^{(2)}(t, t')$ , by

$$g^{(2)}(t, t') \equiv \frac{I(t|t')I(t')}{I_{ss}^2}. \quad (47)$$

This correlation function describes correlations between photon emissions but does not depend on the detector efficiency  $\eta$  with which events are registered. It can therefore be measured very accurately, even when using imperfect detectors with  $\eta < 1$ .

Assuming the measured signal  $M = g^{(2)}(T, 0)$  we determine the accuracy  $\Delta\varphi$  as a function of the time  $T$  of the measurement stage, by numerically averaging over a relatively large number of quantum trajectories. The results of our simulations are shown in Figs. 7 and 8. As expected, both graphs exhibit a very strong dependence of the system dynamics on the unknown phase,  $\varphi$ . This dependence is most pronounced when  $\varphi = \pi$ . For example, Fig. 8 shows a distinct spike for this angle. In Fig. 7, we observe very large differences between curves whenever  $\varphi$  is close to  $\pi$ , even when  $\varphi$  is only varied by a relatively small amount. Fig. 9 shows the dependence of the phase measurement accuracy  $\Delta\varphi$  on  $T$ , when  $M = g^{(2)}(T, 0)$  and  $\varphi = \pi$ . To calculate this quantity we use again the error propagation formula in Eq. (3). We now find that

$$\Delta\varphi(T) \propto T^{-0.71} \quad \text{for } \varphi = \pi \quad (48)$$

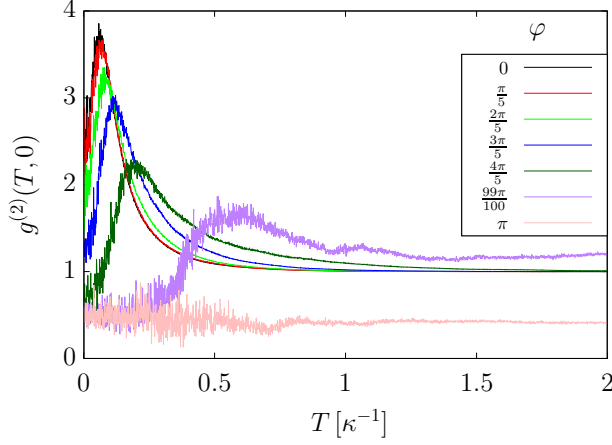


FIG. 7: [Color online] Second-order correlation function  $g^{(2)}(T, 0)$ , as a function of the duration of the measurement stage,  $T$ , for various phases  $\varphi$ . Again we assume  $|\alpha_{ss}|^2 = 4$ ,  $\eta = 0.5$  and averages over  $10^6$  trajectories.

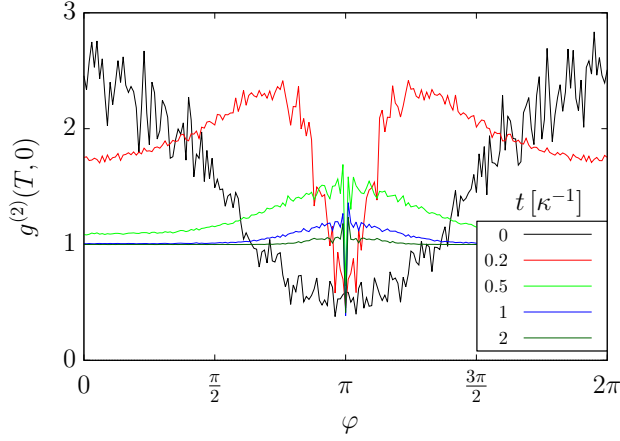


FIG. 8: [Color online] Second-order correlation function  $g^{(2)}(T, 0)$  as a function of the unknown phase,  $\varphi$  for various times,  $T$ , with  $|\alpha_{ss}|^2 = 4$  and  $\eta = 0.5$  averaged over  $10^6$  trajectories.

to a very good approximation. This accuracy clearly beats the standard quantum limit. In other words, second order photon correlation measurements can be very sensitive to phase fluctuations. This is not surprising, since measurements of the second-order photon correlation function  $g^{(2)}(T, 0)$  require the detection of single photons, while intensity measurements can, in principle, be done without high-resolution single-photon detection. This provides us with a quantum element other than entanglement.

A more standard method of resource counting in quantum metrology is to consider the average number of photons that passed through the unknown phase,  $\varphi$ , as the resource,  $N$ . This measure can also be used within our quantum metrology scheme. Using again quantum

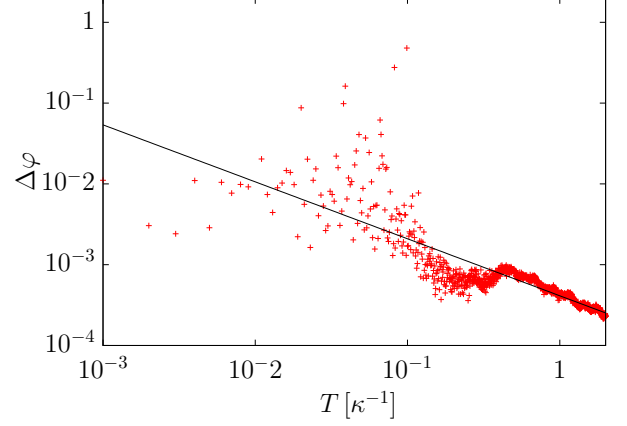


FIG. 9: [Color online] Accuracy  $\Delta\varphi$  of the proposed metrology scheme as a function of the duration of the measurement stage,  $T$ , for measurements of the second-order correlation function  $g^{(2)}(T, 0)$  around  $\varphi = \pi$  to maximise the sensitivity of the proposed scheme. As before, we assume  $|\alpha_{ss}|^2 = 4$ ,  $\eta = 0.5$  and average over  $10^6$  trajectories. The black line shows the approximate solution in Eq. (48).

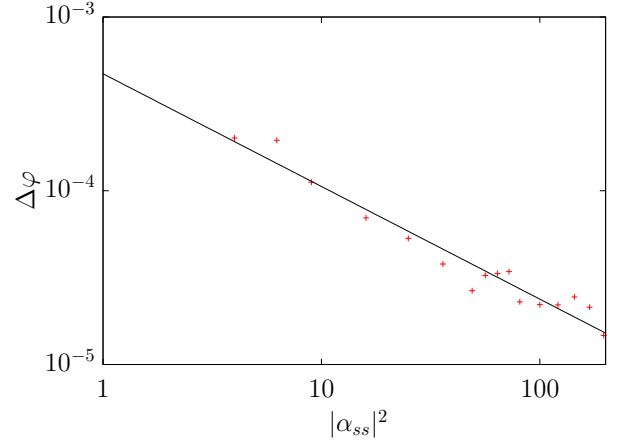


FIG. 10: [Color online] Accuracy,  $\Delta\varphi$ , of the proposed metrology scheme as a function of the initial mean photon number,  $|\alpha_{ss}|^2$ , for measurements of the second-order correlation function  $g^{(2)}(T, 0)$  and  $\varphi = \pi$ . Here,  $\eta = 0.5$  and we average over  $10^6$  trajectories. To remove noisy fluctuations in the signal in time, we take a sample of uncertainties over a fixed period of time, find the average uncertainty in that period and compare this average to the same time average for other initial states. The black line shows the approximate solution in Eq. (49).

jump simulations and the error propagation formula from Eq. (3) with  $M = g^{(2)}(T, 0)$  and averaging over many quantum trajectories, we now calculate the dependence of  $\Delta\varphi$  on the average population of the initial coherent state inside the cavity,  $|\alpha_{ss}|^2$ . The result is shown in Fig. 10. For the parameters that we consider here, we

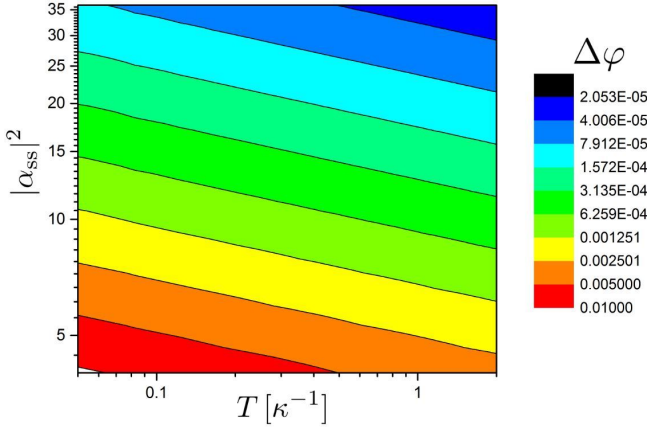


FIG. 11: [Color online] Log-Log plot of the accuracy,  $\Delta\varphi$ , when both the duration of the measurement stage,  $T$ , and the initial mean number of photons,  $|\alpha_{ss}|^2$ , is taken into account and the second order correlation function  $g^{(2)}(T, 0)$  is analysed. Here we have  $\eta = 0.5$  and we consider  $10^6$  repetitions of the experiment.

find that

$$\Delta\varphi(|\alpha_{ss}|^2) \propto (|\alpha_{ss}|^2)^{-0.65} \quad \text{for } \varphi = \pi \quad (49)$$

to a very good approximation. Again, Eq. (48) clearly illustrates a quantum enhancement beyond the standard quantum limit. In practical applications, it might be best to consider both the duration of the measurement stage and the number of photons that passed through the sample as a resource. The result of the simulation of the corresponding experiment is shown in Fig. 11. When we have two scalable resources, our scheme allows more freedom in gaining a highly accurate result, even when one of the resources may be constrained. The measurement uncertainty  $\Delta\varphi$  exceeds the standard quantum limit in both cases.

## V. CONCLUSIONS

In this paper, we propose a quantum-enhanced metrology scheme to measure an unknown phase  $\varphi$ , between two pathways of light with an accuracy beyond the standard quantum limit, given in Eq. (1). Our scheme is based on a laser-driven optical cavity, which is placed inside an instantaneous quantum feedback loop, as illustrated in Fig. 1. The measurement process includes two main steps. Firstly, during the preparation stage, a continuous laser experiences the phase shift,  $\varphi$ , before entering the cavity field. Its purpose is to prepare the cavity in a state that depends strongly on this phase. Secondly, during the measurement phase, the cavity only experiences the quantum feedback loop. Whenever a photon is detected to leak out of the resonator, a laser pulse is activated and displaces the state of the cavity in a controlled way.

In this paper we have assumed that the detector which monitors the cavity during the measurement stage determines its second order correlation function  $g^{(2)}(T, 0)$ . This means, we propose to measure the conditional probability for the detection of a photon in a small time interval  $(T, T + \Delta t)$  after the detection of a photon at the end of the preparation stage. As shown in Section IV B with the help of quantum jump simulations, this second order correlation function can indeed be used to determine  $\varphi$  with a very high accuracy. For the parameters, which we consider as an example, we find that  $\Delta\varphi$  scales as  $T^{-0.71}$  (c.f. Eq. (48)), where  $T$  denotes the duration of the measurement stage. If we consider instead the mean number of photons seen by the unknown phase during the preparation stage as the main resource for our quantum metrology scheme, we find that the accuracy  $\Delta\varphi$  scales as  $(|\alpha_{ss}|^2)^{-0.65}$  (c.f. Eq. (49)). In both cases, we observe an accuracy  $\Delta\varphi$ , which is better than can be achieved classically according to Eq. (1).

In contrast to other quantum metrology schemes [24], our scheme does *not* require entanglement as a resource. The above described quantum enhancement comes instead from the very rich dynamics of the cavity field inside an instantaneous feedback loop, with feedback in the form of displacement pulses. As shown in Section III, the field inside the resonator always remains in a coherent state. The cavity field never reaches a stationary state. Instead, the intensity of the emitted photons might even grow exponentially in time. The dynamics exhibited by the cavity is almost chaotic and depends very strongly on the initial state of the resonator [36].

During the measurement stage, the continuous driving of the cavity is replaced by a feedback loop. This assumption simplifies the analysis of our scheme and might also simplify its experimental realisation. For simplicity, we assume here that the feedback pulses are instantaneous, i.e. that the feedback laser excites the cavity on a time scale that is much shorter than the time scale given by the spontaneous cavity decay rate  $\kappa$ . Implementing the proposed quantum-enhanced metrology scheme in its current form therefore requires a relatively good optical cavity. However, it is well justified to speculate that our proposed quantum metrology scheme also exhibits some quantum enhancement if this condition is not strictly met. To further increase the accuracy of the proposed phase measurements beyond the standard quantum limit, one could measure higher-order photon correlation functions [37, 38].

The main advantage of the quantum metrology scheme, which we propose here, is that its experimental realisation is relatively straightforward. As mentioned already above, we do not require highly-entangled many-photon states as a resource. Furthermore, our scheme does not require highly efficient single photon detectors, since  $g^{(2)}(T, 0)$  can be measured very accurately with detector efficiencies  $\eta < 1$ . High-quality optical cavities are already available in many laboratories worldwide (see for example Refs. [50, 51]). We therefore believe that our

quantum metrology scheme will be of significant practical interest until technologies for the generation of highly-entangled many-photon states become more readily available.

*Acknowledgements.* We thank C. C. Gerry, P. A. Knott,

B. Maybee, F. Torzewska and G. Vitiello for stimulating and helpful discussions. Moreover, we acknowledge financial support from the UK EPSRC-funded Oxford Quantum Technology Hub for Networked Quantum Information Technologies NQIT.

- 
- [1] F. Wolfgramm, C. Vitelli, F. A. Beduini, N. Godbout and M. W. Mitchell, *Entanglement-enhanced probing of a delicate material system*, Nature Photon. **7**, 28-32 (2013).
  - [2] M. A. Taylor, J. Janousek, V. Daria, J. Knittel, B. Hage, H.-A. Bachor and W. P. Bowen, *Biological measurement beyond the quantum limit*, Nature Photon. **7**, 229 (2013).
  - [3] A. Crespi, M. Lobino, J. C. F. Matthews, A. Politi, C. R. Neal, R. Ramponi, R. Osellame and J. L. O'Brien, *Measuring protein concentration with entangled photons*, Appl. Phys. Lett. **100**, 233704 (2012).
  - [4] V. Giovannetti, S. Lloyd and L. Maccone, *Quantum-enhanced measurements: beating the standard quantum limit*, Science **306**, 1330 (2004).
  - [5] V. Giovannetti, S. Lloyd and L. Maccone, *Quantum metrology*, Phys. Rev. Lett. **96**, 010401 (2006).
  - [6] M. Zwiernik, C. A. Perez-Delgado and P. Kok, *Ultimate limits to quantum metrology and the meaning of the Heisenberg limit*, Phys. Rev. A **85**, 042112 (2012).
  - [7] B. L. Higgins, D. W. Berry, S. D. Bartlett, H. M. Wiseman and G. J. Pryde, *Entanglement-free Heisenberg-limited phase estimation*, Nature **450**, 393 (2007).
  - [8] C. M. Caves, *Quantum-mechanical noise in an interferometer*, Phys. Rev. D **23**, 1693 (1981).
  - [9] R. S. Bondurant and J. H. Shapiro, *Squeezed states in phase-sensing interferometers*, Phys. Rev. D **30**, 2548 (1984).
  - [10] H. Lee, P. Kok and J. P. Dowling, *A Quantum Rosetta Stone for Interferometry*, J. Mod. Opt. **49**, 2325 (2002).
  - [11] R. A. Campos, C. C. Gerry and A. Benmoussa, *Optical interferometry at the Heisenberg limit with twin Fock states and parity measurements*, Phys. Rev. A **68**, 023810 (2003).
  - [12] J. Joo, W. J. Munro and T. P. Spiller, *Quantum metrology with entangled coherent states*, Phys. Rev. Lett. **107**, 083601 (2011).
  - [13] C. C. Gerry, J. Mimih and R. Birrittella, *State-projective scheme for generating pair coherent states in traveling-wave optical fields*, Phys. Rev. A **84**, 023810 (2011).
  - [14] P. A. Knott, W. J. Munro and J. A. Dunningham, *Attaining subclassical metrology in lossy systems with entangled coherent states*, Phys. Rev. A **89**, 053812 (2014).
  - [15] S. D. Huver, C. F. Wildfeuer and J. P. Dowling, *Entangled Fock states for Robust Quantum Optical Metrology, Imaging, and Sensing*, Phys. Rev. A **78**, 063828 (2008).
  - [16] K. Jiang, C. J. Brignac, Y. Weng, M. B. Kim, H. Lee and J. P. Dowling, *Strategies for choosing path-entangled number states for optimal robust quantum-optical metrology in the presence of loss*, Phys. Rev. A **86**, 013826 (2012).
  - [17] D. W. Berry and H. M. Wiseman, *Optimal states and almost optimal adaptive measurements for quantum interferometry*, Phys. Rev. Lett. **85**, 5098 (2000).
  - [18] C. C. Gerry, *Heisenberg-limit interferometry with four-wave mixers operating in a nonlinear regime*, Phys. Rev. A **61**, 043811 (2000).
  - [19] C. C. Gerry and J. Mimih, *The parity operator in quantum optical metrology*, Contemp. Phys. **51**, 497 (2010).
  - [20] A. De Pasquale, P. Facchi, G. Florio, V. Giovannetti, K. Matsuoka and K. Yuasa, *Two-Mode Bosonic Quantum Metrology with Number Fluctuations*, Phys. Rev. A **92**, 042115 (2015).
  - [21] R. Carranza and C. C. Gerry, *Photon-subtracted two-mode squeezed vacuum states and applications to quantum optical interferometry*, JOSA B **29**, 2581 (2012).
  - [22] K. Macieszczak, M. Guta, I. Lesanovsky and J. P. Garrahan, *Dynamical phase transitions as a resource for quantum enhanced metrology*, arXiv:1411.3914 (2014).
  - [23] S. Alipour, M. Mehboudi and A. T. Rezakhani, *Quantum Metrology in Open Systems: Dissipative Cramer-Rao Bound*, Phys. Rev. Lett. **112**, 120405 (2014).
  - [24] J. P. Dowling and K. P. Seshadreesan, *Quantum Optical Technologies for Metrology, Sensing, and Imaging*, J. Lightwave Technol. **33**, 2359 (2015).
  - [25] P. Kok, H. Lee and J. P. Dowling, *The creation of large photon-number path entanglement conditioned on photodetection*, Phys. Rev. A **65**, 052104 (2002).
  - [26] The LIGO Scientific Collaboration, *A gravitational wave observatory operating beyond the quantum shot-noise limit*, Nature Phys. **7**, 962 (2011).
  - [27] J. Aasi et al., *Enhanced sensitivity of the LIGO gravitational wave detector by using squeezed states of light*, Nature Photon. **7**, 613 (2013).
  - [28] K. R. Motes, J. P. Olson, E. J. Rabeaux, J. P. Dowling, S. J. Olson and P. P. Rohde, *Linear Optical Quantum Metrology with Single Photons: Exploiting Spontaneously Generated Entanglement to Beat the Shot-Noise Limit*, Phys. Rev. Lett. **114**, 170802 (2015).
  - [29] H. M. Wiseman and G. J. Milburn, *Quantum Measurement and Control*, Cambridge University Press, ISBN: 978-0-521-80442-4.
  - [30] V. Giovannetti, P. Tombesi and D. Vitali, *Non-Markovian quantum feedback from homodyne measurements: The effect of a nonzero feedback delay time*, Phys. Rev. A **60**, 1549 (1999).
  - [31] Y. Yamamoto, N. Imoto, and S. Machida, *Amplitude squeezing in a semiconductor laser using quantum non-demolition measurement and negative feedback*, Phys. Rev. A **33**, 3243 (1986).
  - [32] C. Sayrin, I. Dotsenko, X. Zhou, B. Peaudecerf, T. Rybarczyk, S. Gleyzes, P. Rouchon, M. Mirrahimi, H. Amini, M. Brune, J.-M. Raimond and S. Haroche, *Real-time quantum feedback prepares and stabilizes photon number states*, Nature **477**, 73 (2011).
  - [33] G. Kiesslich, C. Emary, G. Schaller and T. Brandes, *Reverse quantum state engineering using electronic feedback loops*, New J. Phys. **14**, 123036 (2012).

- [34] C. Emary, *Delayed feedback control in quantum transport*, Phil. Trans. R. Soc. A **371**, 1999 (2013).
- [35] L. A. Clark, W. Huang, T. M. Barlow and A. Beige, *Hidden Quantum Markov Models and Open Quantum Systems with Instantaneous Feedback* in ISCS 2014: Interdisciplinary Symposium on Complex Systems, Emergence, Complexity and Computation **14**, p. 143, Springer (2015).
- [36] L. A. Clark, B. Maybee, F. Torzewska and A. Beige, *Quantum chaos and feedback*, (in preparation).
- [37] S. Oppel, T. Büttner, P. Kok, and J. von Zanthier, *Super-resolving multi-photon interferences with independent light sources*, Phys. Rev. Lett. **109**, 233603 (2012).
- [38] M. E. Pearce, T. Mehringer, J. von Zanthier and P. Kok, *Precision Estimation of Source Dimensions from Higher-Order Intensity Correlations*, Phys. Rev. A **92**, 043831 (2015).
- [39] H.-P. Breuer and F. Petruccione, *The Theory of Open Quantum Systems*, Oxford University Press, ISBN: 978-0-19-921390-0.
- [40] A. Stokes, A. Kurcz, T. P. Spiller and A. Beige, *Extending the validity range of quantum optical master equations*, Phys. Rev. A **85**, 053805 (2012).
- [41] W. H. Zurek, *Decoherence, einselection, and the quantum origins of the classical*, Rev. Mod. Phys. **75**, 715 (2003).
- [42] J. P. Paz and W. H. Zurek, *Quantum Limit of Decoherence: Environment Induced Superselection of Energy Eigenstates*, Phys. Rev. Lett. **82**, 5181 (1999).
- [43] G. Lindblad, *On the generators of quantum dynamical semigroups*, Comm. Math. Phys. **48**, 119 (1976).
- [44] G. C. Hegerfeldt, *How to reset an atom after a photon detection: Applications to photon-counting processes*, Phys. Rev. A **47**, 449 (1993).
- [45] J. Dalibard, Y. Castin, and K. Mølmer, *Wave-function approach to dissipative processes in quantum optics*, Phys. Rev. Lett. **68**, 580 (1992).
- [46] H. Carmichael, *An Open Systems Approach to Quantum Optics*, Lecture Notes in Physics, Volume **18** (Springer, Berlin, 1993).
- [47] D. B. Khoroshko and S. A. Kilin, *Suppression of photocurrent shot noise in a feedback loop*, J. Exp. Theor. Phys. **79**, 691 (1994).
- [48] Y. M. Golubev, I. V. Sokolov, and M. I. Kolobov, *Possibility of suppressing quantum light fluctuations when excess photon fluctuations occur inside a cavity*, J. Exp. Theor. Phys. **84**, 864 (1997).
- [49] A. V. Masalov, A. A. Putilin and M. V. Vasilyev, *Subpoissonian Light and Photocurrent Shot-noise Suppression in Closed Optoelectronic Loop*, J. Mod. Opt. **41**, 1941 (1994).
- [50] A. Kuhn, M. Hennrich, and G. Rempe, *Deterministic Single-Photon Source for Distributed Quantum Networking*, Phys. Rev. Lett. **89**, 067901 (2002).
- [51] J. McKeever, A. Boca, A. D. Boozer, R. Miller, J. R. Buck, A. Kuzmich and H. J. Kimble, *Deterministic generation of single photons from one atom trapped in a cavity*, Science **303**, 1992 (2004).